Heating Potential of Iron Oxides for Therapeutic Purposes in Interventional Radiology[1]

Ingrid Hilger, PhD, Katrin Frühauf, Wilfried Andrä, PhD, Robert Hiergeist, PhD
Rudolf Hergt, PhD, Werner A. Kaiser, MD, MS

Rationale and Objectives. In addition to their diagnostic applications, iron oxides could be used therapeutically to eliminate tumors with heat if their heating powers are adequate. The authors therefore examined the specific absorption rate (SAR) of different iron oxide (magnetite) samples suspended in water and in liquid or solidified gel.

Materials and Methods. The authors compared two ferromagnetic fine powders (total particle size, >350 nm and 100 nm), five superparamagnetic ferrofluidic samples (total particle size, 10–280 nm), and a commercially available contrast medium (ferumoxides injectable solution, Endorem). The SARs of the magnetic material—suspended in distilled water or in liquid or solid agar—were estimated from time-dependent calorimetric measurements during exposure to an alternating-current magnetic field (amplitude, 6.5 kA/m; frequency, 400 kHz).

Results. SARs varied considerably between the different iron oxide samples. The highest value was found for a ferrofluidic sample (>93 W/g), while Endorem had little heating power (<0.1 W/g). The SAR was clearly dependent on the aggregation state of the matrix only for the large-particle–size ferromagnetic sample, yielding the highest values for particle suspensions in water (74 W/g) and lowest for solid agar (8 W/g). The heating power of the smaller-particle–size ferromagnetic sample did not exceed 8 W/g.

Conclusion. Heating powers differed according to the interaction of multiple physical parameters. Iron oxides should be selected carefully for therapeutic applications in magnetic heating.

Key Words. Hyperthermia; iron; neoplasms, therapy, magnetic thermoablation.

The application of iron oxides for diagnostic procedures has gained wide acceptance in radiologic practice (1–3), but therapeutic applications are still under investigation. Such applications have exploited two major advantages of iron oxides: their low toxicity to human beings (4) and their magnetization. For example, the magnetization is used to target drugs to the tumor area through external static magnetic fields (5). The tumor elimination is confined to the coupled cytotoxic drugs. If exposed to an alternating magnetic field, the harmless iron oxide particles become powerful heat sources by transforming the energy from the magnetic field into heat. Gilchrist et al (6) first proposed such an application, and several approaches are currently under investigation for the treatment of tumors. One is called magnetic hyperthermia and involves the generation of temperatures up to 45°–47°C with iron oxides as particles (7) or as seeds (8). The treatment works by rendering cells more sensitive to radiation therapy or chemotherapy. Another technique, called magnetic thermoablation (9), employs temperatures above 47°C, which have strong cytotoxic effects on both tumor and normal cells. The use of particles allows the deposi-

Acad Radiol 2002; 9:198–202

[1] From the Department of Diagnostic and Interventional Radiology, Klinikum der Friedrich-Schiller-Universität Jena, Bachstrasse 18, D-07740 Jena, Germany (I.H., K.F., W.A.K.); and the Institut für Physikalische Hochtechnologie e.V., Jena, Germany (W.A., R. Hiergeist, R. Hergt). Received July 24, 2001; revision requested October 1; revision received and accepted October 9. **Address correspondence to** I.H.

Features of the Magnetic Materials Used in the Present Study

Sample	Type*	Shape	Total Particle Diameter (nm)	Magnetite Core Diameter (nm)	Coating	Coercive Force (kA/m)
1	Powder	Crushed	>350†	>350†	None	3
2	Powder	Crushed	100†	100†	None	≅30‡
3	Ferrofluid	Spheroid	10†	8§	Organic components, anionic surfactant	0
4	Ferrofluid	Spheroid	200§	3–10‡	Starch	0
5	Ferrofluid	Spheroid	280§	3–10‡	Starch	0
6	Ferrofluid	Spheroid	125§	3–10‡	Starch	0
7	Ferrofluid	Spheroid	150§	3–5§	Dextran	0

*Ferrofluids are water-based colloidal suspensions of coated magnetic particles.
†Measurements determined by means of transmission electron microscopy.
‡Values estimated according to the manufacturing procedure.
§Measurements provided by the supplier.

tion of iron oxides to be restricted to the tumor area (eg, by intratumoral injection), thereby avoiding adverse systemic effects.

The heating of magnetic oxides in an alternating-current magnetic field is due mainly to loss processes during reorientation of the magnetization (10) or frictional losses with particle rotations in low-viscous environments (11). A large heating power is desirable to reduce the material amount to be administered to the patient. For a reliable dosage, the heating power of the magnetic particles—commonly called the specific absorption rate (SAR) and describing the energy amount converted into heat per time and mass—has to be investigated thoroughly. Therefore, we determined the heating potential of various commercially available prototype iron oxide samples. The magnetic material comprised both magnetic fine powders and ferrofluid samples, which are colloidal suspensions of coated particles. Because particle immobilization can occur in different molecular structures of the tumor area (eg, cellular membranes, proteins), the magnetic material was suspended in media in different states.

MATERIALS AND METHODS

Iron Oxide Samples

The iron oxide samples were purchased from Heraeus (Hanau, Germany; sample 1), Ferrofluidics (Nürtingen, Germany; sample 3), or Guerbet (Sulzach, Germany; ferumoxides injectable solution, Endorem, sample 7) or provided by Chemicell GmbH (Berlin, Germany; samples 4–6, patent DE 196 24 426 A1). Sample 2 was prepared from sample 1 by grinding for about 300 hours. The features of these magnetic materials are summarized in the Table. Particle sizes and shapes were determined by means of scanning electron microscopy. With the exception of Endorem, the investigated magnetic samples have not been tested for human applications. All iron oxide samples were chemically composed of nontoxic magnetite (Fe_3O_4).

Suspension Media

For SAR determinations, the iron oxide samples were suspended in media in different states, with studies including aqueous suspensions and suspensions in liquid and solid agar. The aqueous suspensions included 0.1 g of samples 1 and 2 per milliliter of distilled water. The ferrofluid aqueous suspensions were measured as delivered without addition of distilled water. The liquid agar suspensions included 0.1 g of samples 1 and 2 and 0.1 mL of samples 3–7 per milliliter of liquid agar. The 2% wt/vol agar solutions were measured in a liquid state after being heated to 50°C by a water-bath controlled thermostat. The mixtures were stirred during the calorimetric measurements (see below) to maintain a homogeneous particle suspension. For solid agar suspensions, identical particle concentrations were suspended in hot liquid agar, stirred until they cooled to the gelling point, and then measured in the solid state.

Determination of Iron Oxide Mass in Ferrofluids

For the ferrofluidic samples (samples 3–7), the iron oxide mass (m_i) was determined by assuming that the ferrofluids are composed mainly of water and iron oxides and that the mass of the iron oxides is much larger than that of the particle coatings (see Discussion). After 10-fold weight determinations of defined ferrofluid volumes,

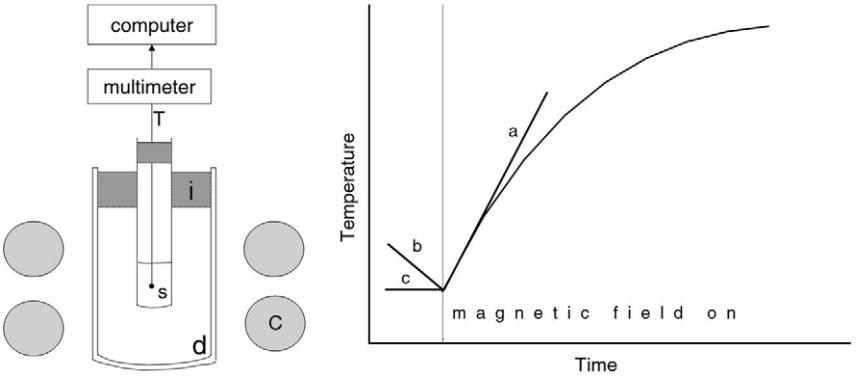

Figure 1. Calorimetric determination of the SAR of suspended iron oxide samples. **(a)** Experimental setup. *T* = thermosensor, *I* = isolation, *s* = suspended iron oxide particles, *d* = vacuum vessel (dewar), *c* = magnetic field inductor coil. **(b)** Schematic temperature curves. Lines *a* and *b* are regression lines for the determination of temperature-to-time variations in Equation (2) (see Materials and Methods), with *b* the regression line before magnetic field exposure of iron oxide suspensions that are not thermically equilibrated and *c* the temperature course before magnetic field exposure of thermically equilibrated suspensions.

the formulas $m_{ff} = m_w + m_i$, $V_{ff} = V_w + V_i$, and $\delta = m/V$ (where m_{ff} is the mass of the ferrofluid, m_w is the mass of water, m_i is the mass of iron oxide, V_{ff} is the volume of ferrofluid, V_w is the volume of water, V_i is the volume of iron oxide, and δ is the density) were used to give the expression

$$m_i = \delta_i \cdot \frac{(m_{ff} - \delta_w \cdot V_{ff})}{\delta_i - \delta_w}, \qquad (1)$$

where δ_i and δ_w are the densities of iron oxide and water, respectively, for the final calculation of the iron oxide mass.

Calorimetric Determination of the SAR

For the calorimetric determination of the SAR, the iron oxide suspensions were thermally isolated in a vacuum vessel (dewar) and placed into a circular coil (diameter, 9 cm; two turns). To measure temperature changes over time during exposure to an alternating magnetic field (amplitude, 6.5 kA/m; frequency, 400 kHz), we used a thermocouple of copper and constantan wires (0.09 mm and 0.16 mm in diameter, respectively) connected to a multimeter with automatic registration (Keithley, Germering, Germany). In control experiments, the heating of the thermocouple without iron oxide samples was found to be negligible. The selection of the magnetic field parameters was restricted by the technical limits of the available device (EFD Induktionserwärmung Fritz Düsseldorf GmbH, Freiburg, Germany) with a nominal output power of 5 kW. The nominally inductive coil was matched to the output impedance of the power amplifier by the manufacturer. The magnetic field amplitude was measured with a pickup coil of known turn number and area by means of an oscillograph.

The corresponding experimental setup is shown schematically in Figure 1a. From measured time-dependent temperature curves, the temperature-to-time variation for the start of heating ($\Delta T/\Delta t$) was calculated from regression line *a* as shown schematically in Figure 1b. For thermally equilibrated samples (aqueous solutions of iron oxide particles, suspensions in solid agar) with steady temperatures before exposure to an alternating magnetic field (line *c* in Fig 1b), the SAR was calculated by the following formula:

$$\mathrm{SAR} = (c \cdot m_s \cdot \Delta T/\Delta t)/m_i, \qquad (2)$$

where *c* is the specific heat capacity of the sample, m_i is the total iron oxide mass in the suspension, m_s is the mass of the sample mixture, *T* is the temperature, and *t* is time. This means that the data were normalized with respect to the magnetite mass. In prototype experiments, the specific heat capacities of solid and liquid agar were found to be comparable to that of water. For samples that were not thermally equilibrated (those requiring heating to maintain agar in a liquid state) $\Delta T/\Delta t$ from regression line *a* was corrected by the temperature variation with time, as expressed by the slope of regression line *b*. All experiments

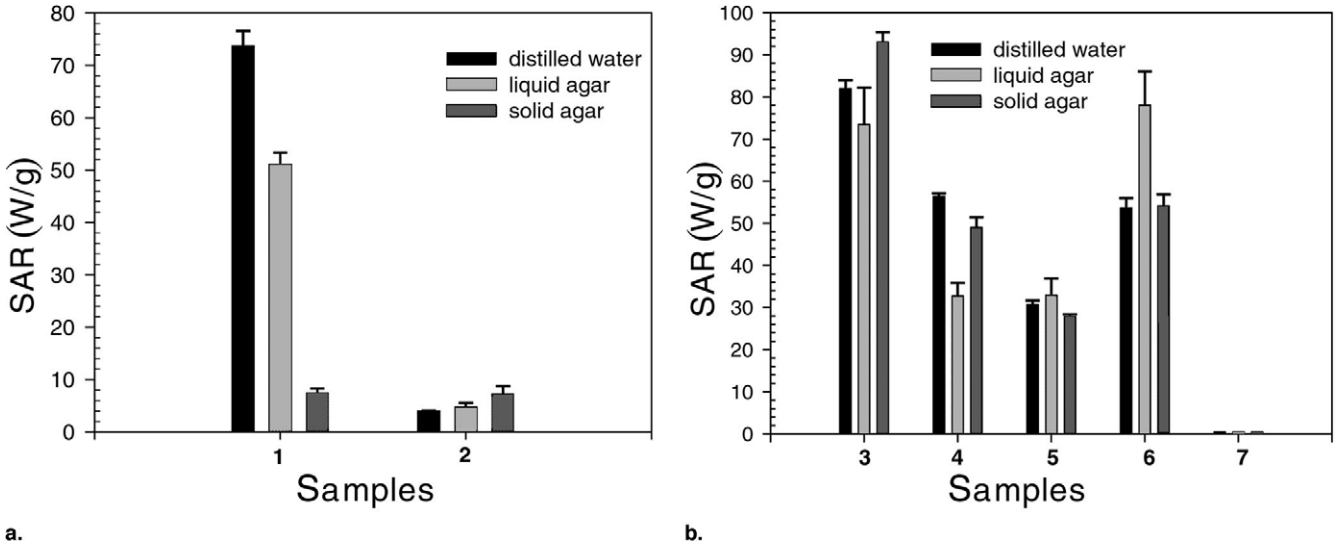

Figure 2. Heating powers of different iron oxide samples, as indicated by the SARs, for a frequency of 400 kHz and a magnetic field amplitude of 6.5 kA/m. **(a)** Iron oxide in fine powder form; sample 2 is produced by grinding sample 1. **(b)** Ferrofluidic samples (colloidal suspension of coated nanoparticles). The samples were suspended in aqueous, liquid (liquid agar), and solid (solid agar) media. Because samples 4–7 violate the precondition of Equation (1), the corresponding SARs represent only lower limits.

were performed in triplicate. Data are presented as means and ± standard deviations of the mean.

RESULTS

Distinct SARs were found for the different samples. Those for samples 1 and 2 are shown in Figure 2a. For sample 1, the SARs differed depending on the states of the suspension medium; the SARs were significantly higher for particles suspended in water (74 W/g) or liquid agar (51 W/g). For particles suspended in solid agar or after grinding, the SARs were comparatively low (<8 W/g).

For the ferrofluidic iron oxide samples, there was no significant correlation between the SAR and the particle suspension medium. Sample 3 had the highest SARs (73–93 W/g), and sample 7, the contrast medium Endorem, showed almost no heating power (<0.1 W/g) for the magnetic field parameters used (Fig 2b).

DISCUSSION

According to our data, the SARs of the different iron oxide samples vary considerably. Prepared by different procedures, the samples differ in particle size and shape (Table), which determine their magnetic properties and consequently their heating power (12).

As mentioned with respect to Equation (1), the iron oxide mass m_i can be calculated with satisfying accuracy only for particles with relatively thin coatings. Otherwise, the actual value of m_i is smaller, and the SAR is higher than calculated. Therefore, the corresponding data for samples 4–7 were only roughly estimated.

The heating potential for samples 1 and 2 in solid agar can be understood by the basis of multidomain particle behavior, which was theoretically predicted for nearly cubic grains with diameters larger than 100 nm (13). According to this theory, heating is generated by domain wall displacement during exposure to an alternating magnetic field. This behavior is typical for ferromagnetic materials. After the particle size of sample 1 was reduced by grinding (to produce sample 2, shown in the Table and Fig 2) the heating potential in liquid medium decreased markedly. Presumably, an increase in the coercivity force with mechanical work occurred (14), and coercivity forces higher than the amplitudes of the alternating-current magnetic field may have reduced the heating power.

The variation in the heating potential of sample 1 with the state of the suspension medium can be explained by the fact that there is an additional contribution to heating produced by particle rotations or vibrations (the so-called rotational losses), which are increasingly inhibited by particle immobilization with increasing cross-linked agarose molecules in the surroundings. Specifically, when agar is heated the cross-links between the galactose polymers are broken, and when it is cooled the cross-links reform (15). This fact suggests that the heating potential of sample 1 in water is generated mainly by rotational losses. The observations with sample 1 exemplify the in vivo situation in which variations

in SARs could reflect the degree of particle immobilization at the tumor area, for example, by bindings between residues of the coating and cellular membranes or matrix proteins. For unknown reasons, however, a comparable dependency was not observed after the grinding of sample 1 and the ferrofluidic samples.

The heating of samples 3–6 is due to relaxational losses occurring from rotation of the particle magnetization vector or mechanical rotation of the entire particle. The heating potential of ferrofluidic sample 7, a contrast medium widely used for the detection of liver lesions with magnetic resonance imaging, was negligible. The diameter of the magnetic core was probably too small for the production of heating due to relaxational losses. Apart from particle size and the magnetic field parameters, many other parameters influence the SAR of a magnetic material, including the particle coating, the agglomeration behavior (12), and others not clearly identified. The precise reasons for the insufficient heating capacity of sample 7 should be clarified in further studies.

In contrast to sample 7, ferrofluidic samples 3–6 showed a broad spectrum of different heating potentials. The magnetic field parameters used in the present study are of particular interest for applications in heating therapy. Because of the relatively high SAR at the examined magnetic field parameters, cytotoxic temperatures could be achieved with minimal iron oxide doses. This finding is important not only because it allows for dose reduction but also because with intratumoral administration the amount of foreign material taken up at the target is limited by interstitial hypertension caused by the lack of functioning lymphatics (16).

As known from clinical applications, iron oxides are taken up by the reticuloendothelial system (17). Even if iron particles are administered locally, there is a risk of systemic uptake and impairment of the reticuloendothelial system due to heating. Therefore, only tumors in parts of the body distant from the reticuloendothelial system should be treated, for example, the breast, head, or limbs.

In summary, our results show that the heating power differed considerably between the iron oxide samples. A contrast agent approved by the Food and Drug Administration does not produce sufficient heat. Therefore, in selection of materials for heating therapy, the interaction of multiple parameters should be considered. It remains unclear which physical parameters should be chosen to design iron oxide particles with high heating efficiency. Further detailed investigations focusing on loss mechanisms are necessary. This topic is currently under investigation by our group.

ACKNOWLEDGMENTS

The authors thank Doreen Schröder for excellent technical assistance and Christian Bergemann, Dipl-Ing (Chemicell GmbH, Berlin, Germany), for providing ferrofluidic samples.

REFERENCES

1. Nanz D, Weishaupt D, Quick HH, et al. TE-switched double-contrast enhanced visualization of vascular system and instruments for MR-guided interventions. Magn Reson Med 2000; 43:645–648.
2. Saini S, Sharma R, Baron RL, et al. Multicentre dose-ranging study on the efficacy of USPIO ferumoxtran-10 for liver MR imaging. Clin Radiol 2000; 55:690–695.
3. Bellin MF, Beigelman C, Precetti-Morel S. Iron oxide-enhanced MR lymphography: initial experience. Eur J Radiol 2000; 34:257–264.
4. Marchal G, van Heke P, Demaerel P, et al. Detection of liver metastases with superparamagnetic iron oxide in 15 patients: results of MR imaging at 1.5 T. AJR Am J Roentgenol 1989; 152:771–775.
5. Lübbe AS, Bergemann C, Riess H, et al. Clinical experiences with magnetic drug targeting: a phase I study with 4′-epidoxorubicin in 14 patients with advanced solid tumors. Cancer Res 1996; 56:4686–4693.
6. Gilchrist RK, Medal R, Shorey WD, et al. Selective inductive heating of lymph nodes. Ann Surg 1957; 146:596–606.
7. Jordan A, Scholz R, Wust P, et al. Magnetic fluid hyperthermia (MFH): cancer treatment with AC magnetic field induced excitation of biocompatible superparamagnetic nanoparticles. J Magnetism Magn Mat 1999; 201:413–419.
8. van Wieringen N, Kotte AN, van Leeuwen GM, et al. Dose uniformity of ferromagnetic seed implants in tissue with discrete vasculature: a numerical study on the impact of seed characteristics and implantation techniques. Phys Med Biol 1998; 43:121–138.
9. Hilger I, Hergt R, Kaiser WA. Effects of magnetic thermoablation in muscle tissue using iron oxide particles: an in vitro study. Invest Radiol 2000; 35:170–179.
10. Kneller E. Theory of the magnetization curve of small crystals. In: Wijn HP, ed. Ferromagnetism: encyclopedia of physics series. Vol XVIII/2. New York, NY: Springer Verlag, 1966; 438–544.
11. Shliomis MI. Magnetic fluids. Sov Phys Usp 1963; 17:153–185.
12. Hergt R, Andrä W, d'Ambly CG, et al. Physical limits of hyperthermia using magnetite fine particles. IEEE Trans Magnetics 1998; 34:3745–3754.
13. Butler RF, Banerjee SK. Theoretical single-domain grain size range in magnetite and titanomagnetite. J Geophys Res 1975; 80:4049–4058.
14. Heider F, Dunlop DJ, Sugiura N. Magnetic properties of hydrothermally recrystallized magnetite crystals. Science 1987; 236:1287–1290.
15. Bickerstaff GF. Department of Biological Sciences, University of Paisley home page. Available at: *http://www-biol.paisley.ac.uk/courses/stfunmac/glossary/agarose.html*. Accessed March 26, 2001.
16. Less JR, Posner MC, Boucher Y, et al. Interstitial hypertension in human breast and colorectal tumors. Cancer Res 1992; 52:6371–6374.
17. Saini S, Stark D, Hahn PF, et al. Ferrite particles: a superparamagnetic MR contrast agent for the reticuloendothelial system. Radiology 1987; 162:211–216.